



BUILDING PREDICTIVE MODELS TO ASSESS DEGRADATION OF SOIL ORGANIC MATTER OVER TIME USING REMOTE SENSING DATA

Abdulsalam Mashaal Faisal Aljumaily, Ammar Younes Ahmed Kashmoola

Department of Soil Sciences and Water Resources, College of Agriculture and Forestry, University of Mosul, Iraq.

ABSTRACT

Article information
Article history:
Received:19/10/2022
Accepted:1/11/2022
Available:31/12/2022

Keywords:

predictive models, organic matter, soil, remote sensing.

DOI:

<https://10.33899/magj.2022.136537.1204>

Correspondence Email:

abdulsalam.faisal@uomosul.edu.iq

Agricultural fields near Rabia district, northwest of Nineveh Governorate/Iraq, were selected for study, as the study area is located between longitudes (36°31'51.34" and 36°43'40.343") north and two latitudes (42°16'14.475" and 42°34'50.99") east, with an area of approximately 52.5 hectares. The predictive model is built from the integration of multiple linear and nonlinear regression relationships between remote sensing data and laboratory-measured organic matter concentration values. The predictive model was applied to Satellite data for three years (2002, 2012, and 2022), producing three maps to describe the soil content of organic matter (a map for each year). The results of the study showed the possibility of applying predictive models to Satellite data for a particular area and for previous years to give results with high spatial accuracy ($R^2 = 0.9581$). Spatial maps were possible for each of the three years studied (2002, 2012, and 2022), and fertility maps were drawn by projecting spectral evidence values into the predictive model equation in the ENVI program. The resulting images were then processed using ArcGIS 10.8 to color them and perform a Reclassify operation and take them out with the values of percentages of organic matter concentrations. The results showed a clear deterioration in the soil's organic matter content over time, especially between 2012 and 2022.

College of Agriculture and Forestry, University of Mosul.

This is an open access article under the CC BY 4.0 license (<https://magj.mosuljournals.com/>).

INTRODUCTION

The diagnosis and estimation of the amount of organic matter, the degree of reaction, the salt concentration and the necessary ready-made elements are fertility tests necessary to assess the productivity of agricultural land, and by the difference and variability we obtain compared to previous years it is possible to assess the amount of deterioration in soil fertility (Adamu et al., 2014). The integration of remote sensing data with laboratory test values enabled Prudnikova et al. (2021) to build predictive models that enable them to prepare numerical maps of some of the chemical properties of the soil. The use of remote sensing data and their mathematical relationships with the numerical values of laboratory tests of the chemical properties of the soil enabled Taha et al. (2014) to prepare digital maps for the distribution of nitrate and ammonium concentrations in the soils of the northern parts of Babylon Governorate using the outputs of remote sensing data represented by spectral evidence (SAVI, OSAVI, GDVI).

Some of the fertility soil traits of previous years in a row and the preparation of digital maps can be predicted by integrating laboratory tests with remote sensing

data into predictive models, linear and non-linear regression formulas, with a spatial accuracy superior to conventional maps (Wang et al., 2021).

In this study, we can construct predictive models resulting from exponential, linear and logarithmic relationships between the values of spectral evidence (SI, VARI, FMI) and the results of laboratory tests of organic matter.

MATERIALS AND METHODS

Study area and area.

The agricultural fields near Rabia district, northwest of Nineveh Governorate/Iraq, were selected as the area for research, due to the lack of studies on soil fertility using remote sensitization that are specific to this area and their suitability to the nature of The study area was located between (36°31'51.34" and 36°43'40.343") north and the points (42°16'14.475" and 42°34'50.99') east according to GPS readings, and the study location area was 52.5 hectares.

Soil samples collection.

50 composite soil samples were taken, distributed almost regularly over the studied area to be representative of the studied area. The samples were dried, then grinded and sieved with a sieve with a diameter of 2 mm openings and kept in polyethylene bags away from sunlight, then carried out physical and chemical laboratory tests, that including soil reaction, electrical conductivity of soil solution, calcium carbonate, calcium sulfate, organic matter, ready-made nitrogen, ready-made phosphorus, ready-made potassium, dissolved calcium, dissolved magnesium, dissolved sodium, bicarbonate, chlorides (pH, EC, CaCO₃, CaSO₄, OM, N, P, K, CA, MG, Na, HCO₃, Cl) respectively, and I followed the methods adopted for it.

A set of satellite data captured by the Enhanced Thematic Mapper plus (Landsat7) satellite (Landsat7) as well as by the Landsat7 Satellite Enhanced Land Imager and Thermal Infrared Sensor 2 Level-1 (Operational Land Imager and Thermal Infrared Sensor Collection 2 Level-1) were used, and the Path and row for this statement is (170 and 35) respectively. The three satellite visualizations were taken on dates (12/02/2002, 4/2/2012 and 7/2/2022).

Using ENVI 5.3, space images were processed within the FLAASH Fast Line of sight Atmospheric Analysis of Spectral Hypercube model to remove atmospheric effects and deduct the study area from the aerial image (Mruthyunjaya et al., 2022). Exponential and logarithmic values of spectral evidence were calculated to test the relationship of spectral evidence values with the laboratory-measured fertility concentrations of the study samples, resulting in the selection of the following spectral evidence:

1. Salinity Index (SI) (Khan and Abbas, 2007):

$$SI = \text{Green}^2 + \text{Red}^2 + \text{NIR}^2 \dots\dots\dots (1)$$

2. Ferrous Minerals Index (FMI) (Storey et al., 2014):

$$FMI = (\text{SWIR1} / \text{NIR}) \dots\dots\dots (2)$$

3- Visible Atmospherically Resistant Index (VARI) (Gitelson et al., 2022):

$$VARI = (\text{Green} - \text{Red}) / (\text{Green} + \text{Red} - \text{Blue}) \dots\dots\dots (3)$$

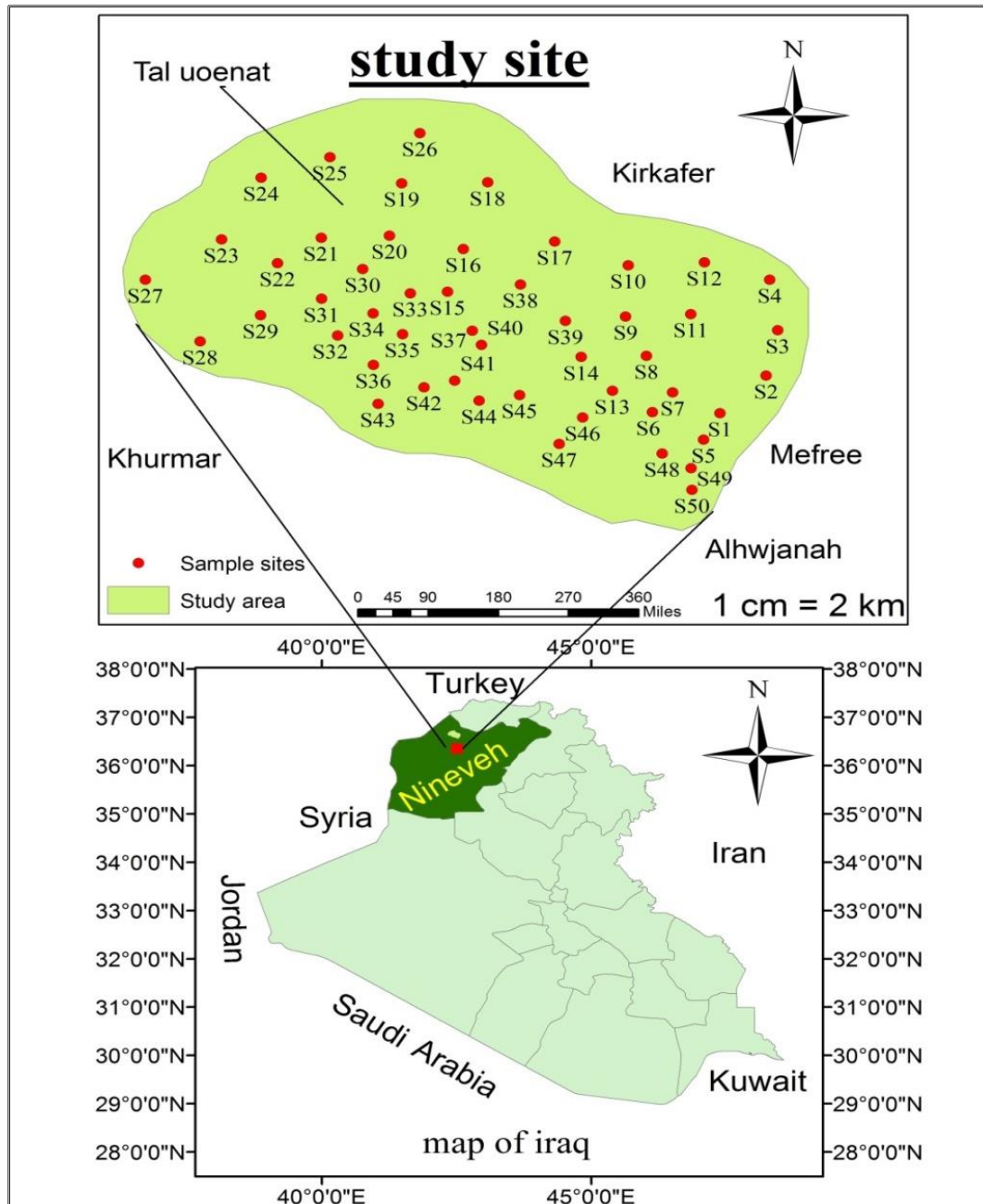


Figure (1): A map showing the study site.

SPSS and Excel were used to calculate the value of the determination coefficient R^2 to find statistical relationships between some variables, as well as organize tables, perform mathematical calculations, and prepare graphs to illustrate the differences between study sites.

After finding the values of the evidence that were affected by the reflectivity of organic matter and extracted using ArcGIS 10.8, then a correlation and regression analysis were performed and the exponential and logarithmic relationships were tested using SPSS 21 between the values of the selected evidence and the results of the laboratory analysis of the concentration of organic matter to find the relationship between them that will represent the predictive model equation that will be applied to space visuals for the years 2002, 2012 and 2022 in order to represent the fertility status of those years on color maps using Kriging and Reclassify technology in ArcGIS software.

After the spectral evidence values at each site of the sample taken were extracted, using ENVI 5.3, these values were arranged in special tables corresponding to the names and numbers of the samples taken at them, and then the exponential, linear, and logarithmic relationships of these values were tested with the concentration of organic matter in the study samples. The correlation between organic matter concentration on the one hand and spectral evidence values and exponential, linear and logarithmic relationship values was studied using SPSS and resulted in more than one predictive model and each model having a different degree of accuracy value (R^2).

The most accurate predictive model was selected based on the value of (R^2). The following predictive model was elected, in which the relationship accuracy was ($R^2 = 0.9581$):

$$OM = - 6.828 + 0.005 * (VARI) + 6.767 * \text{Exp} (SI) + 0.483 * (FMI) \dots\dots\dots (4)$$

After we obtained the predictive model above, its value was calculated, and the results were very close to the concentration of organic matter measured in the laboratory for the samples of the study area, through which it was relied on to draw maps describing the concentration of organic matter for the three years studied using the program ENVI 5.3 and then the resulting images were processed using the program Arcmap 10.8 to distinguish it in colors and perform the process of reclassify and take it out with the values of percentages of the limits of concentrations of organic matter.

The percentage of organic matter in the soil is classified into three categories:

Low : O.M. < 1 %

Medium :O.M. ranged between 1% - 2%

High :O.M. > 2 %

RESULTS AND DISCUSSION

The results of the application of the predictive model of organic matter (equation 4) showed high accuracy in describing the distribution of organic matter ratios over the study area ($R^2=0.9581$) and there was a significant relationship between the concentrations of laboratory-measured organic matter and the values of spectral evidence. The status of organic matter in 2002 and 2012 was possible to be predicted by applying the predictive model to the space data of those years, and the amount of deterioration in the amount of organic matter in the study area was observed over time. These findings were consistent with what researchers Prudnikova and Savin (2021) found when studying the state of organic matter through remote sensing data.

The results in Figure (2) show a decrease in soil content of organic matter over time in terms of the decline in the area of the High variety during the years 2012-2022 and 2022-2012 by 20.5% and 20.6% for each of the two periods respectively. While the area of the Medium variety increased between 2002 and 2012 and 2022 by 35.7% and 16% for the two years respectively, there was no space within the study area located within the Low variety until 2022 to consist of 4% of the area of the total study area.

The reason for the lack of organic matter over time can be due to the decrease in agricultural activity over time in the study area compared to previous years, as the area was characterized by large and diverse agricultural activities as indicated by the people of the region and workers in the Agriculture Division of Rabia district, although organic matter may be depleted with the stressful agricultural activity of the

soil, leaving the land barren increases the chance of its annual exposure to high temperatures that cause its content of the substance to decrease Membership (Foth and Ellis, 2018).

From the maps shown in Figure (3), we can observe the distribution of organic matter ratios over the study area within the three classes referred to (Low, Medium and High) and the heterogeneity in these ratios between the years 2002 to 2022. These findings are consistent with the findings of researchers Ali and Taha (2017) and Taha et al. (2014) in their studies, where they were able to observe the quantitative degradation of soil organic matter content using predictive models obtained from remote sensing data.

Table (2): Physical and chemical qualities measured in vitro.

Sample No.	texture	Av.N ppm	Av.P ppm	Av.K ppm	CEC mq/100g	O.M. g.Kg ⁻¹	CaSO ₃ g.Kg ⁻¹	CaCO ₃ g.Kg ⁻¹	EC dS/m	pH
1	SL	34.6	10.91	137.3	35.90	27.5	22	330	4.68	7.2
2	C	36.37	10.14	148.07	34.28	18.9	27.1	335	3.22	7.2
3	SL	32.47	12.83	157.50	43.78	29.2	19.8	265	4.97	7.3
4	CL	32.36	11.42	142.44	40.43	22.4	18.9	325	2.92	7.3
5	CL	35.88	10.04	134.45	39.34	16.5	24.6	235	3.04	7.3
6	CL	36.55	11.36	107.81	41.41	12	22.5	260	2.34	7.2
7	CL	33.23	13.52	197.84	38.05	20.6	24.2	225	1.46	7.3
8	SCL	35.47	10.58	111.79	39.05	10.3	21.7	260	2.92	7.3
9	SC	31.95	11.41	123.53	39.76	25.8	15	100	3.39	7.2
10	SCL	34.3	9.74	52.55	30.81	18.9	12.5	110	4.39	7.2
11	SCL	30.12	16.19	249.41	32.59	24.1	24.2	190	4.09	7.2
12	SCL	34.54	11.52	170.13	27.52	27.5	24.2	150	3.22	7.3
13	L	33.35	12.73	173.92	37.41	17.2	22	220	5.38	7.3
14	L	32.66	10.82	113.79	39.07	17.9	16.2	255	4.39	7.3
15	L	32.44	10.87	143.16	40.04	13.8	19.1	235	3.51	7.3
16	L	36.93	10.13	123.51	44.00	8.6	26	250	2.92	7.3
17	L	37.72	10.01	91.88	36.84	17.2	23.8	250	2.63	7.3
18	L	35.64	10.15	160.85	42.88	19.9	27.3	215	3.63	7.3
19	CL	32.51	12.29	142.17	35.95	25.8	19	210	3.39	7.2
20	SL	33.17	9.99	92.54	35.37	24.1	1.2	220	2.92	7.2
21	L	36.62	10.48	107.22	28.99	18.9	23.7	205	2.34	7.4
22	L	35.07	9.52	14.50	36.85	31.6	9.5	210	2.81	7.3
23	L	36.9	9.68	93.55	34.90	25.8	22.5	225	3.8	7.4
24	L	32.17	12.6	211.33	37.45	20.6	25.4	220	4.68	7.4
25	L	29.07	14.72	233.9	40.78	17.2	20.4	115	1.17	7.4
26	L	31.36	13.93	201.61	29.23	15.5	21.5	175	2.92	7.3
27	L	33.68	9.98	77.64	45.40	21.3	14.5	195	2.34	7.3
28	L	35.23	9.73	121.70	46.76	19.9	22.5	155	3.22	7.3
29	SCL	34.35	9.29	97.71	37.01	17.2	18.4	195	4.09	7.2
30	SCL	35.76	10.78	173.49	36.20	13.8	28.2	190	3.63	7.2
31	SCL	35.62	10.72	137.22	39.90	16.5	24.4	195	4.97	7.2
32	SCL	35.22	11.36	113.26	40.42	22.4	21	220	4.68	7.2
33	SCL	19.69	10.72	818.99	48.88	27.5	29.5	230	2.81	7.3
34	SL	35.19	10.5	145.75	33.91	6.9	24.6	200	3.22	7.2
35	SCL	36.26	10.25	130.49	39.94	17.2	24.2	180	4.68	7.2

36	SCL	35.42	11.14	131.48	42.52	13.8	23.7	185	2.92	7.3
37	SCL	34.44	10.44	132.12	35.94	18.9	22.1	215	4.79	7.2
38	SCL	29.2	18.77	255.89	45.99	24.1	22.4	145	3.51	7.2
39	SCL	33.54	10.23	151.85	36.23	21.3	21.9	275	2.63	7.4
40	SCL	32.52	11.14	226.18	41.59	29.2	24.5	210	2.92	7.2
41	SCL	32.81	11.37	142.47	43.54	27.5	19.4	155	3.63	7.2
42	L	35.54	9.89	100.99	40.90	16.5	21.5	315	3.8	7.3
43	SCL	32.65	12	173.38	38.22	18.9	21.1	170	2.81	7.2
44	SCL	33.82	9.96	116.89	35.23	27.5	18.4	135	2.05	7.3
45	SL	35.1	10.06	133.23	48.75	17.2	23	155	3.51	7.2
46	L	36.61	10.55	117.11	36.85	28.2	24	115	1.75	7.3
47	SCL	35.52	10.31	174.77	31.41	20.6	26.5	180	4.39	7.2
48	SCL	34.25	10.12	174.64	42.67	15.5	24.2	185	3.22	7.3
49	SL	35.6	10.33	132.77	37.53	17.2	23.9	255	4.09	7.3
50	L	36.59	10.95	158.57	35.37	21.3	28.7	190	4.68	7.3

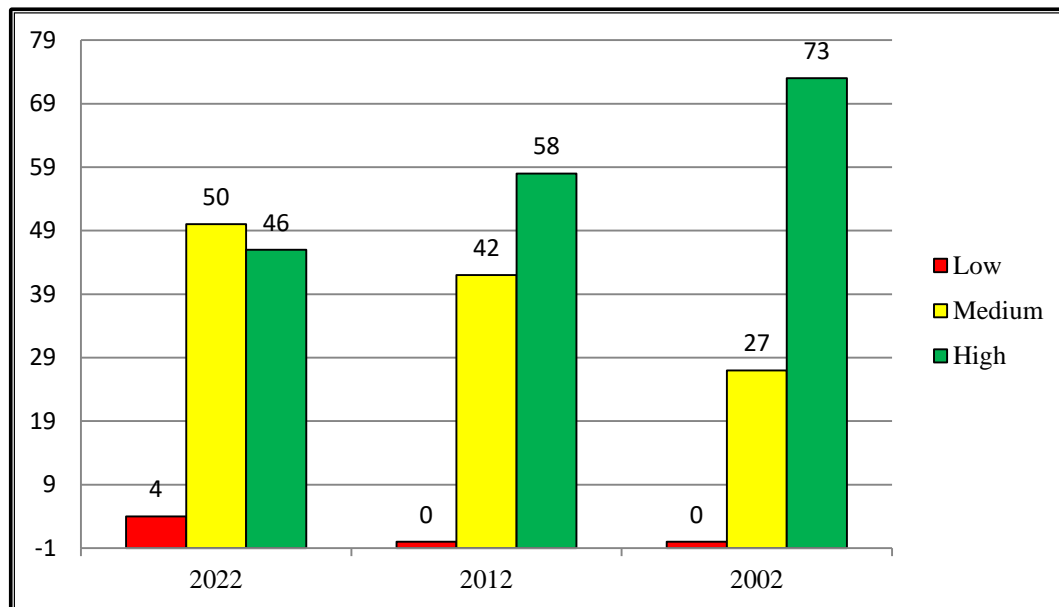
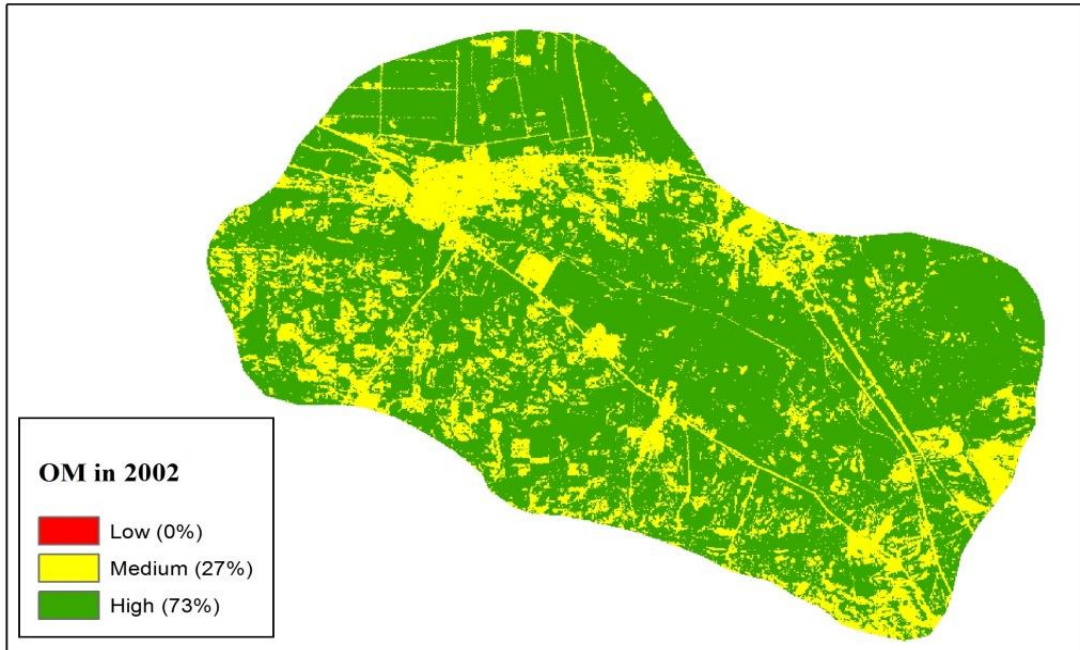


Figure (2): Percentages of the area of organic matter (O.M. %) varieties in the years studied.

These findings also agreed with the findings of Nascimento et al. (2021) when studying to observe and evaluate the degradation of soil traits using remote sensing data in the state of São Paulo, Brazil, where they were able to assess the state of degradation in the soil in terms of its content of organic matter and other qualities over time over thirty-five years, and also were able through their study to find a guide to soil fertility and condition highly dependent on organic matter, and the results of our study approached in terms of the relationship of spectral reflectivity. The amount of organic matter in the soil is largely with the results of their study.

The decline in the soil content of organic matter in the study area during the last two decades, if anything, indicates mismanagement in the proper exploitation of land resources, in addition to the fact that the region suffers from the migration of farmers to it or their abandonment of the agricultural profession, as a result of several factors, including the lack of support of the local farmer with seeds and fertilizer that are primarily good

to contribute to the reconstruction of the land, and the lack of demand for the GDP and many other factors.



Figure(3-a): Percentages of the areas according to the range of organic matter ratios in the studied location in year 2002.

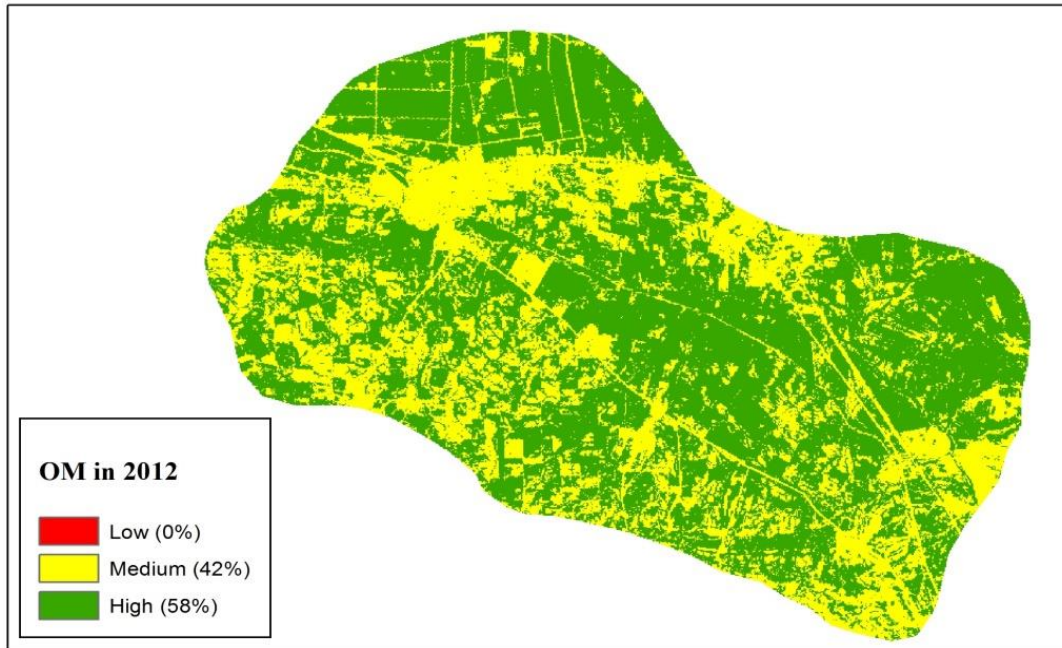


Figure (3-b): Percentages of the areas according to the range of organic matter ratios in the studied location in year 2012.

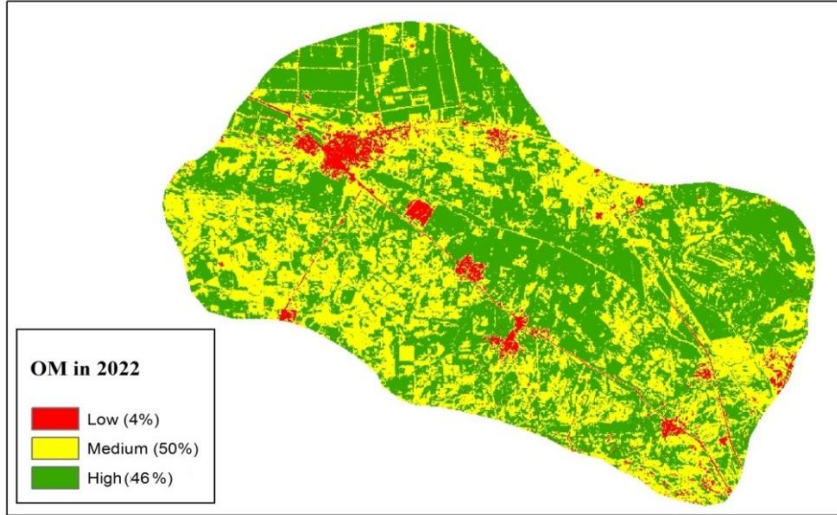


Figure (3:c): Percentages of the areas according to the range of organic matter ratios in the studied location in year 2022.

CONCLUSIONS

The results of the study showed us that the predictive model has a high potential in estimating the amount of organic matter in the soil and gives high-accuracy results close to the results of laboratory testing, and we found a significant decrease in the soil content of organic matter during the past twenty years.

ACKNOWLEDGMENT

The authors are very grateful to the University of Mosul, College of Agriculture and Forestry for the facilities they provided and which helped to improve the quality of this work.

CONFLICT OF INTEREST

None of the authors has a financial or personal relationship with other people or organizations that could inappropriately influence or bias the content of the paper.

بناء موديلات تنبؤية لتقييم التدهور في المادة العضوية في التربة عبر الزمن باستخدام بيانات التحسس
النائي

عبد السلام مشعال فيصل الجميلي

عمار يونس احمد كشمولة

قسم علوم التربة والموارد المائية، كلية الزراعة والغابات، جامعة الموصل، نينوى، العراق.

الخلاصة

تم اختيار حقول زراعية قريبة من ناحية ربيعة شمال غرب محافظة نينوى/ العراق للدراسة، إذ تقع منطقة الدراسة بين خطي طول (36°31'51" و 36°43'40") شمالاً ودائرتي عرض (24°16'47" و 42°34'50") شرقاً، وقد بلغت مساحتها ما يقارب 52.5 هكتاراً (210 كم²). تم بناء الموديل التنبؤي من تكامل علاقات الانحدار الخطية وغير الخطية المتعددة بين بيانات التحسس النائي وقيم تركيز المادة العضوية المقاسة مختبرياً. طُبّق الموديل التنبؤي على البيانات الفضائية للسنوات الثلاث

(2002 و 2012 و 2022)، لتنتج لنا ثلاث خرائط لوصف محتوى التربة من المادة العضوية (خارطة لكل عام). وأظهرت نتائج الدراسة مكانية تطبيق الموديلات التنبؤية على بيانات فضائية لمساحة معينة ولسنوات سابقة لتعطي نتائج بدقة مكانية عالية بلغت ($R^2 = 0.9581$). أمكن رسم خرائط مكانية لكل عام من الأعوام الثلاثة المدروسة (2002 و 2012 و 2022)، وقد تم رسم الخرائط الخصوبية من خلال اسقاط قيم الأدلة الطيفية في معادلة الموديل التنبؤي في برنامج ENVI. ومن ثم تم معالجة الصور الناتجة وذلك باستخدام برنامج Arc map 10.8 لتميزها بالألوان وإجراء عملية إعادة التصنيف (Reclassify) وإخراجها مع قيم النسب المئوية لحدود تراكيز المادة العضوية. وبينت النتائج وجود تدهور واضح في محتوى التربة من المادة العضوية بمرور الزمن خاصة بين العامين 2012 و 2022.

كلمات مفتاحية: موديلات تنبؤية، المادة العضوية، التربة، التحسس النائي.

REFERENCES

- Adamu, G. K., Yusuf, M. A., & Ahmed, M. (2014). Soil degradation in drylands. *Academic Research International*, 5(1), 78. [http://www.savap.org.pk/journals/ARInt./Vol.5\(1\)/2014\(5.1-10\).pdf](http://www.savap.org.pk/journals/ARInt./Vol.5(1)/2014(5.1-10).pdf)
- Ali, H. S., & Taha, A. M. (2017). Quantitative assessment for soil chemical degradation using remote sensing data. *Iraq Journal of Agricultural Research*, 22(7). <https://www.iasj.net/iasj/article/150849>
- Foth, H. D., & Ellis, B. G. (2018). Soil fertility. *CRC Press*. <https://doi.org/10.1201/9780203739341>
- Khan, S., & Abbas, A. (2007). Using remote sensing techniques for appraisal of irrigated soil salinity. *Int. Congr. Model. Simul.(MODSIM), Model. Simul.* New Zealand, Bright, (January), 2632-2638. <https://researchoutput.csu.edu.au/files/9629947/CSU290411.pdf>
- Mruthyunjaya, P., Shetty, A., Umesh, P., & Gomez, C. (2022). Impact of Atmospheric Correction Methods Parametrization on Soil Organic Carbon Estimation Based on Hyperion Hyperspectral Data. *Remote Sensing*, 14(20), 5117. <https://doi.org/10.3390/rs14205117>
- Nascimento, C. M., de Sousa Mendes, W., Silvero, N. E. Q., Poppiel, R. R., Sayão, V. M., Dotto, A. C., ... & Demattê, J. A. (2021). Soil degradation index developed by multitemporal remote sensing images, climate variables, terrain and soil attributes. *Journal of Environmental Management*, 277, 111316. <https://doi.org/10.1016/j.jenvman.2020.111316>
- Prudnikova, E. Y., Savin, I. Y., & Vindeker, G. V. (2021, October). Possibilities of remote sensing monitoring of soil fertility indicators of arable soils. In IOP Conference Series: *Earth and Environmental Science*, 862 (1) 012008. IOP Publishing. <https://n9.cl/40tyi>
- Storey, J., Choate, M., & Lee, K. (2014). Landsat 8 operational land imager on-orbit geometric calibration and performance. *Remote sensing*, 6(11), 11127-11152. <https://doi.org/10.3390/rs61111127>
- Wang, Z., Zhang, F., Zhang, X., Chan, N. W., Ariken, M., Zhou, X., & Wang, Y. (2021). Regional suitability prediction of soil salinization based on remote-sensing derivatives and optimal spectral index. *Science of the Total Environment*, 775, 145807. <https://doi.org/10.1016/j.scitotenv.2021.145807>